第34卷 第4期
2019年4月

地球科学进展
ADVANCES IN EARTH SCIENCE

Vol.34 No.4
Apr.，2019

张为，周丽，唐红峰，等.水热体系中Na_2SO_4/K_2SO_4溶解度的热力学计算[J].地球科学进展，2019，34(4)：414-423.DOI：10.11867/j.issn.1001-8166.2019.04.0414.[Zhang Wei，Zhou Li，Tang Hongfeng，et al. Thermodynamic calculation of solubility of Na_2SO_4/K_2SO_4 in hydrothermal fluids [J]. Advances in Earth Science，2019，34(4)：414-423. DOI：10. 11867/j. issn. 1001-8166. 2019. 04. 0414.]

水热体系中Na_2SO_4/K_2SO_4溶解度的热力学计算*

张 为[1,2]，周 丽[2*]，唐红峰[2]，李和平[2]，王 力[2,3]

（1.贵州师范大学喀斯特生态文明研究中心，贵州 贵阳 550025；2.中国科学院地球化学研究所地球内部物质高温高压院重点实验室，贵州 贵阳 550002；3.中国科学院大学，北京 100039）

摘 要：硫酸盐流体是自然界中的常见热液，其盐度可以为成矿流体演化、成矿元素的迁移富集和矿床类型的划分等提供重要信息。但是现有文献报道的Na_2SO_4和K_2SO_4溶解度多是在饱和蒸气压条件或超临界条件下，而对于低温成矿热液体系的实验研究较少。热力学计算是研究流体性质的重要手段，特别是在实验结果较少的温压范围内起着重要作用，但是利用热力学模型来计算硫酸盐溶解度的工作却少有开展。使用Pitzer模型，利用Na_2SO_4和K_2SO_4溶液高温高压条件下的密度数据，使用非线性最小二乘法拟合，获得了压力对Na_2SO_4和K_2SO_4的活度系数及其溶解过程中的标准偏摩尔体积影响的模型参数，评价了压力对其活度系数和标准偏摩尔体积的影响。结合文献中饱和蒸气压下的相关参数，构建了温度范围为0~250 ℃，压力范围为0.1~40.0 MPa，Na_2SO_4和K_2SO_4溶解度的热力学计算模型。模型计算结果与文献数据吻合较好。计算结果还显示，压力对Na_2SO_4和K_2SO_4的平均活度系数和溶度积都有正向的促进作用，但是由于平均活度系数随压力的变化更大，导致Na_2SO_4和K_2SO_4的溶解度随压力的增大而降低，并且随着温度的升高这种降低的程度变得更大。

关 键 词：硫酸盐流体包裹体；溶解度；热力学计算；Pitzer模型

中图分类号：P592；P595 **文献标志码：**A **文章编号：**1001-8166(2019)04-0414-10

1 引 言

硫酸盐流体是地质流体的一个重要类型，在海陆相各环境中广泛存在[1]，在四川冕宁木落稀土矿床[2]、兰坪金顶超大型铅锌矿床[3]和河南省大河沟锑矿[4]都有发现。流体包裹体是圈闭在矿物晶格缺陷，或其窝穴中保存下来的古流体，是成岩成矿流体的最直观体现[5]。流体包裹体的一项重要研究内容是包裹体盐度的确定[6~9]，成矿热液中硫酸盐(Na_2SO_4/K_2SO_4)溶解度的研究，对反映成矿流体演化过程[10]、矿床类型的划分[11]、流体的氧化还原状态[12]和成矿元素的迁移富集规律[13]具有重要的指示意义。

水热体系中Na_2SO_4/K_2SO_4溶解度的研究已经取得了很多非常重要的成果，但是大部分实验数据的温度范围都是在100 ℃以内[14]，温度在100 ℃以上的数据也多是在饱和蒸汽压条件下[15,16]。另外，由于Na_2SO_4/K_2SO_4等无机超临界流体的特殊性质，化

收稿日期：2018-11-08；**修回日期：**2019-03-19.

* **基金项目：**国家自然科学基金项目“独居石和磷钇矿在热液中溶解行为的实验研究：对U-Th-Pb年龄有效性以及稀土元素成矿的约束”(编号：41773058)；贵州省科技厅—贵州师范大学联合基金项目“石阡县地热资源可持续利用研究”(编号：黔科合LH字[2017]7339号)资助.

作者简介：张为(1988-)，男，湖北武汉人，讲师，主要从事水—岩反应相关的地球化学研究. **E-mail：**zhangwei@gznu.edu.cn

* **通信作者：**周丽(1980-)，男，湖北潜江人，副研究员，主要从事高温高压实验地球化学研究. **E-mail：**zhouli@vip.gyig.ac.cn

学家们研究了超临界条件下（温度≥374 ℃、压力≥22 MPa）Na_2SO_4和K_2SO_4的溶解度，并给出了计算其溶解度的相关经验模型[17~19]。但是对于温度≤250 ℃的低温热液矿床内的硫酸盐流体性质的研究很少。

热力学计算是模拟物质迁移转化、成矿流体演化，及成矿流体热力学性质最常用也是最强有力的工具之一[20~23]，特别是在实验结果较少的温压范围内起着重要的作用，且在H_2O，NaCl-H_2O以及NaCl-H_2O-CO_2流体热力学性质方面已经取得了丰硕的成果[24,25]。Greenberg等[26]和Pabalan等[27]总结了文献中Na_2SO_4和K_2SO_4体系的溶解度等热力学数据，利用Pitzer模型建立了0~250 ℃，饱和蒸汽压下Na_2SO_4和K_2SO_4溶解度计算模型，但是对于更高压力条件下硫酸盐溶解度的研究还很少。因此，本文拟通过热力学计算研究低温热液水热体系中Na_2SO_4和K_2SO_4的溶解度，力图为低温成矿热液中硫酸盐流体包裹体盐度的研究提供一定的指导。

2　理论背景及计算方法

水热体系中Na_2SO_4和K_2SO_4的溶解过程可表示为：

$$Na_2SO_{4(s)} \leftrightarrow 2Na^+ + SO_4^{2-}, \quad (1)$$

$$K_2SO_{4(s)} \leftrightarrow 2K^+ + SO_4^{2-}, \quad (2)$$

与之对应的溶解平衡反应为：

$$K_{Na_2SO_4} = a_{Na^+}^2 \cdot a_{SO_4^{2-}} = \left(m_{Na}\gamma_{Na}\right)^2 \cdot \left(m_{SO_4^{2-}}\gamma_{SO_4^{2-}}\right), \quad (3)$$

$$K_{K_2SO_4} = a_{K^+}^2 \cdot a_{SO_4^{2-}} = \left(m_{K}\gamma_{K}\right)^2 \cdot \left(m_{SO_4^{2-}}\gamma_{SO_4^{2-}}\right), \quad (4)$$

式中：$K_{Na_2SO_4}$（或$K_{K_2SO_4}$）表示硫酸盐的溶解平衡常数；a_i，m_i和γ_i（i表示Na^+，K^+和SO_4^{2-}）分别表示溶液中物种的活度、质量摩尔浓度和活度系数。为了描述水热体系中Na_2SO_4和K_2SO_4的溶解度，就需要同时获得矿物溶解的溶解平衡常数（K_{sp}）和相关物种的活度系数（γ）。

Pitzer[28]模型被广泛应用于水热体系中物质活度系数的计算[29]，被PHREEQC[30]，GEM-Selektor[31]和ScaleSoftPitzer[32]等世界知名的地球化学计算软件所采用。Greenberg等[26]利用Pitzer模型建立了0~250 ℃，饱和蒸气压下Na_2SO_4和K_2SO_4的溶解度计算模型。但是，Shi等[33]发现不考虑压力情况下重晶石的溶解度要比实验结果低27%，为了准确描述矿物在高温高压下的溶解度就必须考虑压力对活度系数和溶解平衡常数的影响[34]。

2.1　压力对溶解平衡常数和活度系数的影响

溶解平衡常数随压力的变化可表示为[35~37]：

$$\ln K_{sp}(T,P) = \ln K_{sp}\left(T,P_0\right) - \frac{\Delta_r V^0}{RT}\left(P - P_0\right), \quad (5)$$

式中：$K_{sp}(T,P)$和$K_{sp}\left(T,P_0\right)$分别为目标温度压力下和参考压力下的溶解平衡常数；P和T分别表示体系的压力和温度，P_0表示参考压力，当温度低于100 ℃时，P_0=0.1 MPa；当温度高于100 ℃时，P_0表示水的饱和蒸汽压；R为理想气体常数；$\Delta_r V^0$是溶解反应过程中偏摩尔体积的变化。对于Na_2SO_4（或K_2SO_4）而言：

$$\Delta_r V^0 = V^0\left(Na_2SO_4,aq\right) - V^0\left(Na_2SO_4,s\right), \quad (6)$$

式中：$V^0\left(Na_2SO_4,aq\right)$是溶解反应生成物$Na^+$和$SO_4^{2-}$的标准偏摩尔体积之和，$V^0\left(Na_2SO_4,s\right)$是固体$Na_2SO_4$（或$K_2SO_4$）的标准偏摩尔体积。25 ℃和0.1 MPa时，$Na_2SO_4$和$K_2SO_4$的标准偏摩尔体积分别为53.33和65.5 cm^3/mol[38]，且可以不考虑固体矿物的体积随温度压力的变化[37]。

依据Pitzer模型，高压下溶质的活度系数可依据饱和蒸汽压时的活度系数计算[39,40]：

$$\begin{aligned}\ln\gamma(P) = {} & \ln\gamma\left(P_{sat}\right) - \left[A_\phi(P) - A_\phi\left(P_{sat}\right)\right] \\ & \times\left[\frac{\sqrt{I}}{1+b\sqrt{I}} + \frac{2}{b}\ln\left(1+b\sqrt{I}\right)\right] \\ & + 2m\left\{\beta^{(0)v} + \beta^{(1)v}\left(2/\alpha^2 I\right)\left[1-\left(1+\alpha\sqrt{I}\right)\right.\right. \\ & \left.\left.\times\exp\left(-\alpha\sqrt{I}\right)\right]\right\}\left(P - P_{sat}\right) + 3m^2 C^v\left(P - P_{sat}\right), \quad (7)\end{aligned}$$

式中：$\gamma(P)$和$\gamma(P_{sat})$分别为目标压力和饱和蒸汽压下的活度系数；P和P_{sat}分别为目标压力和饱和蒸汽压力；A_ϕ是Debye-Hückel系数；m为溶质的质量摩尔浓度，I为溶液的离子强度；$\beta^{(0)v}$，$\beta^{(1)v}$和C^v分别表示Pitzer模型参数$\beta^{(0)}$，$\beta^{(1)}$和C^φ对压力的导数；α =2 $kg^{1/2}\cdot mol^{1/2}$，b = 1.2 $kg^{1/2}$。

2.2　高温高压下溶解平衡常数和活度系数的计算

Pitzer模型表示的是物种的吉布斯自由能，经过适当的微分可以得到焓、热容和体积（密度）等性质。相反也可以利用热容、焓和密度等数据来评价温度、压力对模型参数的影响[41]。电解质溶液的密度可以用来计算压力对电解质的偏摩尔体积和Pitzer模型表示的溶质的活度系数的影响[20,40]。

电解质的表观摩尔体积可以表示为[36]：

$$V_\varnothing = \frac{1}{m}\left(\frac{1000 + mM_s}{\rho_{sol}} - \frac{1000}{\rho_0}\right), \quad (8)$$

式中：$V_\varnothing$表示电解质的表观摩尔体积（apparent molar volume，cm^3/mol）；m是电解质的质量摩尔浓度（mol/

kg H_2O)；M_s是电解质的摩尔质量(g/mol)；ρ_{sol}和ρ_0分别为目标温度压力下溶液和纯水的密度(g/cm^3)；其中纯水的密度依据IAPWS97方程来计算[42]。

结合Pitzer模型，电解质的表观摩尔体积可表示为：

$$V_{\varnothing} = V_{\varnothing}^{0} + v|z_{+}z_{-}|A_{v}\left[\ln\left(1 + b\sqrt{I}\right)/2b\right] + 2v_{+}v_{-}mRT(B_{v} + v_{+}z_{+}mC^{v}), \quad (9)$$

$$B_{v} = \beta^{(0)v} + \beta^{(1)v}(2/\alpha^{2}I)\left[1 - \left(1 + \alpha\sqrt{I}\right) \times \exp\left(-\alpha\sqrt{I}\right)\right], \quad (10)$$

式中：$V_{\varnothing}^{0}$是电解质在无限稀溶液中的表观摩尔体积，即电解质的标准偏摩尔体积；B_v，$\beta^{(0)v}$，$\beta^{(1)v}$和C^v分别表示Pitzer参数模型参数压力的参数，且一般可以不考虑压力对$\beta^{(1)v}$的影响[43]。z_+和z_-分别是阳离子和阴离子的电价，v_+和v_-分别是阳离子和阴离子的化学计量数，$v = v_+ + v_-$。A_v是体积Debye-Hückel斜率，依据Bradley等[44]的工作计算得出。I是溶液的离子强度，R = 8.314 cm^3·MPa/(K·mol)。

由于电解质的标准偏摩尔体积$V_{\varnothing}^{0}$随温度快速变化，因此一般采用参考浓度法间接确定其随温度压力的变化情况[45,46]。

依据公式(9)，参考浓度为m_r时溶质的表观摩尔体积为：

$$V_{\varnothing,m_r} = V_{\varnothing}^{0} + v|z_{+}z_{-}|A_{v}\left[\ln\left(1 + b\sqrt{I_{m_r}}\right)/2b\right] + 2v_{+}v_{-}m_{r}RT(\beta^{(0)v} + v_{+}z_{+}m_{r}C^{v})。 \quad (11)$$

将公式(9)减去公式(11)，就可以用参考浓度为m_r时的表观摩尔体积表示任意浓度下溶液的表观摩尔体积：

$$V_{\varnothing,m} = V_{\varnothing,m_r} + v|z_{+}z_{-}|A_{v}\left[\ln\left(1 + b\sqrt{I_{m}}\right)/2b - \ln\left(1 + b\sqrt{I_{m_r}}\right)/2b\right] + 2v_{+}v_{-}RT\left[\beta^{(0)v}\left(m - m_{r}\right) + z_{+}v_{+}C^{v}\left(m^{2} - m_{r}^{2}\right)\right]。 \quad (12)$$

将公式(8)代入到公式(12)中，则：

$$\frac{1000 + mM_{s}}{m\rho_{sol}} - \frac{1000}{m\rho_{0}} = \left[\frac{V\left(m_{r}\right)}{m_{r}} - \frac{1000}{m_{r}\rho_{0}}\right] + v|z_{+}z_{-}|A_{v}\left[\ln\left(1 + b\sqrt{I_{m}}\right)/2b - \ln\left(1 + b\sqrt{I_{m_r}}\right)/2b\right] + 2v_{+}v_{-}RT\left[\beta^{(0)v}\left(m - m_{r}\right) + z_{+}v_{+}C^{v}\left(m^{2} - m_{r}^{2}\right)\right], \quad (13)$$

式中：参考浓度m_r一般选用参与参数拟合的实验数据中浓度的上限值，$V(m_r)$，$\beta^{(0)v}$和C^v是温度和压力的函数；ρ_{sol}和ρ_0分别为目标温度压力下溶液和纯水的密度；A_v，b，$\beta^{(0)v}$等表示的意义如以上所述。同时，利用公式(11)可以反向计算电解质溶液的标准偏摩尔体积：

$$V_{\varnothing}^{0} = \left[\frac{V\left(m_{r}\right)}{m_{r}} - \frac{1000}{m_{r}\rho_{0}}\right] - v|z_{+}z_{-}|A_{v}\left[\ln\left(1 + b\sqrt{I_{m_r}}\right)/2b\right] - 2v_{+}v_{-}m_{r}RT(\beta^{(0)v} + v_{+}z_{+}m_{r}C^{v}), \quad (14)$$

通过以上过程，利用水热体系中电解质溶液的密度数据，可以拟合获得$V(m_r)$，$\beta^{(0)v}$和C^v等参数，依据公式(7)可以评价压力对溶质活度系数的影响，利用公式(14)计算的溶质标准偏摩尔体积和公式(5)可以计算溶质的溶解反应平衡常数随压力的变化，进而依据公式(3)和(4)计算得到水热体系中电解质的溶解度。

Pitzer等[40]利用水热体系中NaCl溶液的热容和焓等热力学数据确定了0~300 ℃，0.1~100.0 MPa，0~6 m范围内NaCl活度系数。Møller[47]确定了0~250 ℃，饱和蒸气压下NaCl的活度系数参数；Mao等[25]利用Pitzer模型确定了水热体系中NaCl标准偏摩尔体积和压力对Pitzer参数影响的参数，将二者结合利用公式(7)，我们计算了水热体系中NaCl的平均活度系数(图1)。从图1可看出，结合饱和蒸汽压下参数与压力积分项计算出来的不同浓度下NaCl的平均活度系数和Pitzer等[40]完整模型参数计算出来的结果吻合得很好，证明了该方法和计算过程的可行性。从图1还可看出，在NaCl溶液体系中，压力对活度系数有较大的影响，活度系数随着压力的升高而增大。

3 高温高压条件下Na_2SO_4和K_2SO_4溶解度的计算

对于水热条件下Na_2SO_4体系的密度实验数据文献已有全面而详实的报道，超过1 000个实验数据跨越温度0~300.0 ℃，压力0.1~80.0 MPa(表1)。关于K_2SO_4体系的密度数据相对较少(表2)。Obšil等[48]和Azizov[58]实验研究了20.0~300.0 ℃，10.0~30.0 MPa条件下K_2SO_4溶液的密度；Ellis[53]和Saluja等[54]研究获得了0~200.0 ℃，0.1~2.0 MPa条件下K_2SO_4溶液的密度。不同来源的K_2SO_4体系密度数据之间具有较好的一致性，其密度数据的跨度范围为0~300.0 ℃，0.1~40.0 MPa。

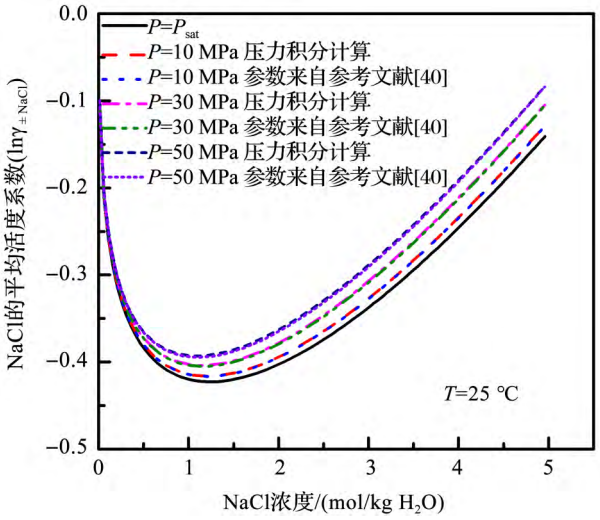

图 1　25 ℃不同压力下，模型计算的 NaCl 的平均活度系数随浓度的变化

Fig. 1　The model calculated NaCl mean activity coefficient at 25 ℃ as a function of concentration under different pressure

表 1　Na_2SO_4-H_2O 体系密度实验数据

Table 1　Summary of density data of Na_2SO_4-H_2O system

温度范围/℃	压力范围/MPa	参考文献
25.0~300.0	9.0~30.0	[48]
25.0~200.0	1.1~68.6	[49]
5.0~60.0	0.1	[50]
20.0~200.0	2.0~10.0	[51]
0~50.0	0.1~80.0	[52]
50.0~200.0	2.0	[53]
25.0~100.0	0.6	[54]
25.0~250.0	0.1~40	[55]
30.0~300.0	2.4~39.8	[56]
5.0~100.0	0.1	[57]

表 2　K_2SO_4-H_2O 体系密度的实验数据

Table 2　Summary of density data of K_2SO_4-H_2O system

温度范围/℃	压力范围/MPa	参考文献
25.0~300.0	9.0~30.0	[48]
50.0~200.0	2.0	[53]
25.0~100.0	0.6	[54]
0~90.0	0.1	[57]
20.0~300.0	5.0~40.0	[58]

对于 Na_2SO_4 和 K_2SO_4 体系，公式(9)和公式(14)转化为：

$$V_{\varnothing} = V_{\varnothing}^{0} + 6A_{\mathrm{v}}\left[\ln\left(1 + \mathrm{b}\sqrt{I}\right)/2\mathrm{b}\right] + 4m\mathrm{R}T\left(\beta^{(0)\mathrm{v}} + 2mC^{\mathrm{v}}\right), \tag{15}$$

$$V_{\varnothing}^{0} = \frac{V(m_{\mathrm{r}})}{m_{\mathrm{r}}} - \frac{1000}{m_{\mathrm{r}}\rho_0} - 6A_{\mathrm{v}}\left[\ln\left(1 + \mathrm{b}\sqrt{I_{m_{\mathrm{r}}}}\right)/2\mathrm{b}\right] - 4\mathrm{R}T\left(m_{\mathrm{r}}\beta^{(0)\mathrm{v}} + 2C^{\mathrm{v}}m_{\mathrm{r}}^{2}\right)。 \tag{16}$$

其中，参考浓度下的摩尔体积和 Pitzer 模型压力参数计算如下：

$$V(m_{\mathrm{r}}) = a_1 + a_2T + a_3T^2 + a_4T^3 + (a_5 + a_6T + a_7T^2)P, \tag{17}$$

$$\beta^{(0)\mathrm{v}} = a_8 + \frac{a_9}{T - 227} + a_{10}T, \tag{18}$$

$$C^{\mathrm{v}} = a_{11} + \frac{a_{12}}{T - 227} + a_{13}T, \tag{19}$$

式中：T 为开尔文温度；P 表示体系的压力，单位为 MPa；a_i 表示模型计算的参数。对于 Na_2SO_4 和 K_2SO_4 体系，利用表 1 和表 2 所列溶液的密度数据，采用非线性最小二乘法，同时拟合获得公式(17)~(19)的参数(表 3)。拟合结果显示，在全部温度压力范围内，模型计算的溶液密度和实验结果的平均偏差分别是 0.057%(Na_2SO_4)和 0.047%(K_2SO_4)，绝大部分实验数据和模型计算的偏差都在 0.1% 以内(图 2)。

表 3　Na_2SO_4 和 K_2SO_4 体积性质计算的参数

Table 3　Parameters for the volumetric properties calculation of Na_2SO_4 and K_2SO_4

参数	Na_2SO_4	K_2SO_4
m_{r}	1.5	1.0
a_1	9.69382688×10^{2}	1.10686112×10^{3}
a_2	2.83105828×10^{-1}	-5.98247606×10^{-1}
a_3	-9.00393580×10^{-4}	5.96259241×10^{-4}
a_4	2.57624184×10^{-6}	2.39804594×10^{-6}
a_5	-1.43199512×10^{0}	-2.71085716×10^{0}
a_6	7.37402186×10^{-3}	1.41493666×10^{-2}
a_7	-1.17539062×10^{-5}	-2.08587301×10^{-5}
a_8	-4.86834961×10^{-4}	5.43596750×10^{-3}
a_9	8.87142143×10^{-2}	4.61245819×10^{-3}
a_{10}	2.75966178×10^{-7}	-1.21299746×10^{-5}
a_{11}	2.13350752×10^{-4}	-5.55380818×10^{-3}
a_{12}	-1.36823713×10^{-2}	6.41685688×10^{-2}
a_{13}	-2.95936943×10^{-7}	1.44544684×10^{-5}

依据公式(16)和表 3 中的参数，我们计算不同温度压力条件下 Na_2SO_4 和 K_2SO_4 的标准偏摩尔体积。计算结果显示，25 ℃和 0.1 MPa 时，模型计算的 Na_2SO_4 和 K_2SO_4 的标准偏摩尔体积分别为 12.26 和 33.42 cm^3/mol，与实验测得的 Na_2SO_4(12.09 cm^3/mol)

和K_2SO_4(33.70 cm^3/mol)[59]的结果吻合得很好。与此同时,我们还计算了Na_2SO_4和K_2SO_4的标准偏摩尔体积随温度压力的变化(图3)。从图3可看出,Na_2SO_4和K_2SO_4的标准偏摩尔体积随温度强烈的变化,在整个温度范围内,随温度的升高而降低,随压力的增大而增大。

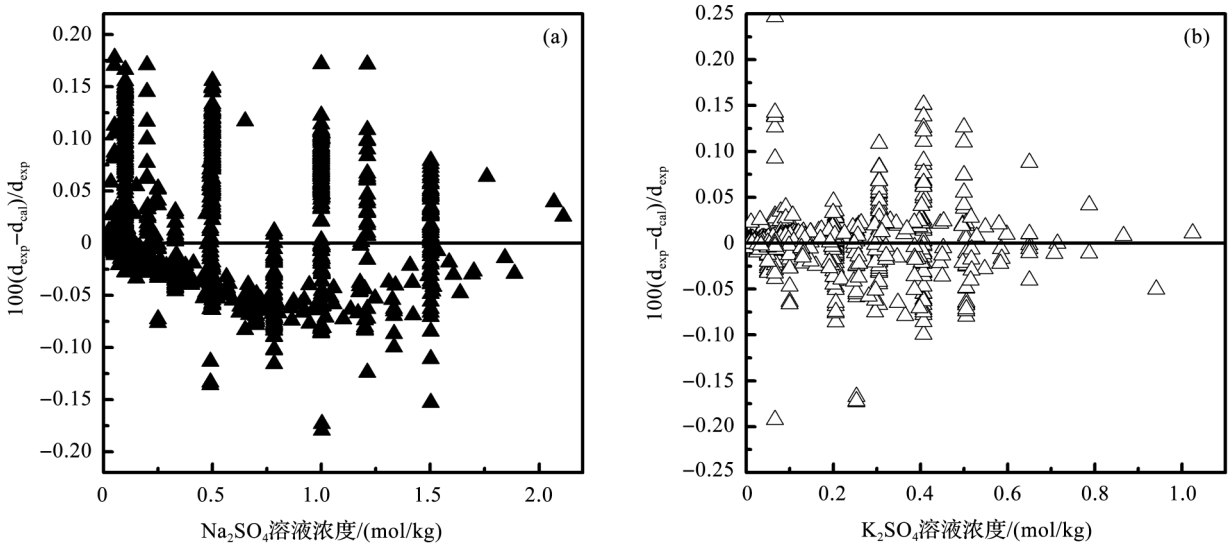

图2 水热体系中模型计算的Na_2SO_4溶液密度(a)和K_2SO_4溶液密度(b)与实验数据的对比

Fig.2 Plot of density deviations between model calculation and literature data of $Na_2SO_4 + H_2O$ (a) and $K_2SO_4 + H_2O$ (b) system

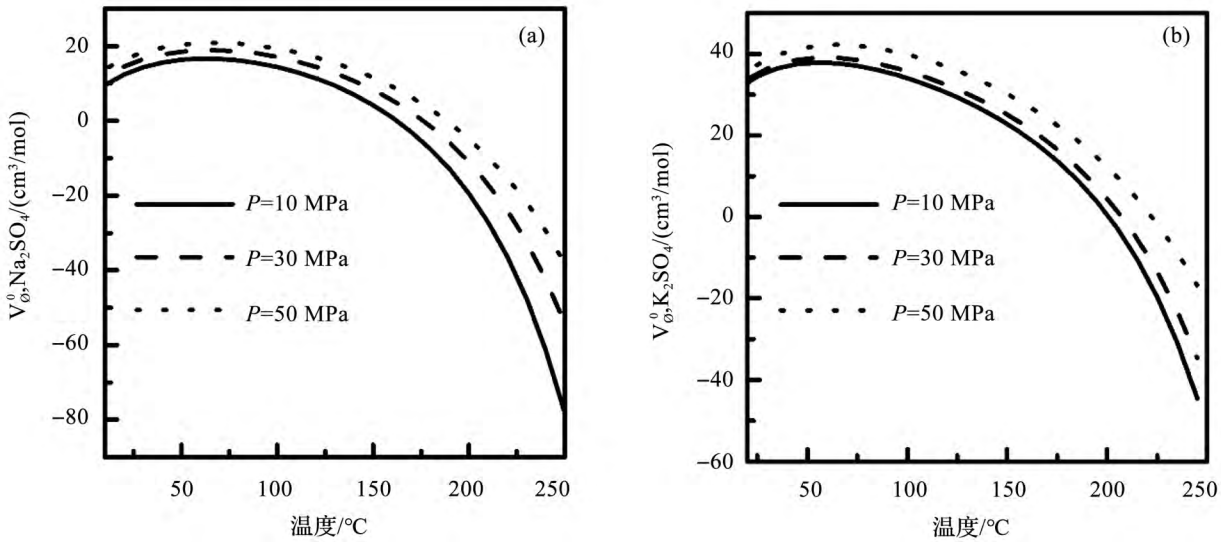

图3 Na_2SO_4(a)和K_2SO_4(b)标准偏摩尔体积随温度的变化

Fig.3 The standard partial molar volumes of Na_2SO_4(a) and K_2SO_4(b) against temperature and pressure

Greenberg等[26]确定了温度0~250 ℃,饱和蒸汽压下Na_2SO_4和K_2SO_4活度系数随温度变化的参数。依据公式(7)和以上获得的参数,我们可以评价压力对Na_2SO_4和K_2SO_4活度系数的影响(图4)。从图4中可以看出,压力的增大会导致Na_2SO_4和K_2SO_4的平均活度系数的增大,并且随着溶液浓度的增大和温度的增高,这种增加的趋势更明显。对于Na_2SO_4体系,250 ℃和30 MPa,1.5 m时Na_2SO_4的平均活度系数比相同温度浓度下,饱和蒸汽压时增加了0.02(图4a);K_2SO_4体系中,250 ℃和30 MPa,0.5 m时的平均活度系数比饱和蒸汽压时增加了0.03(图4b)。

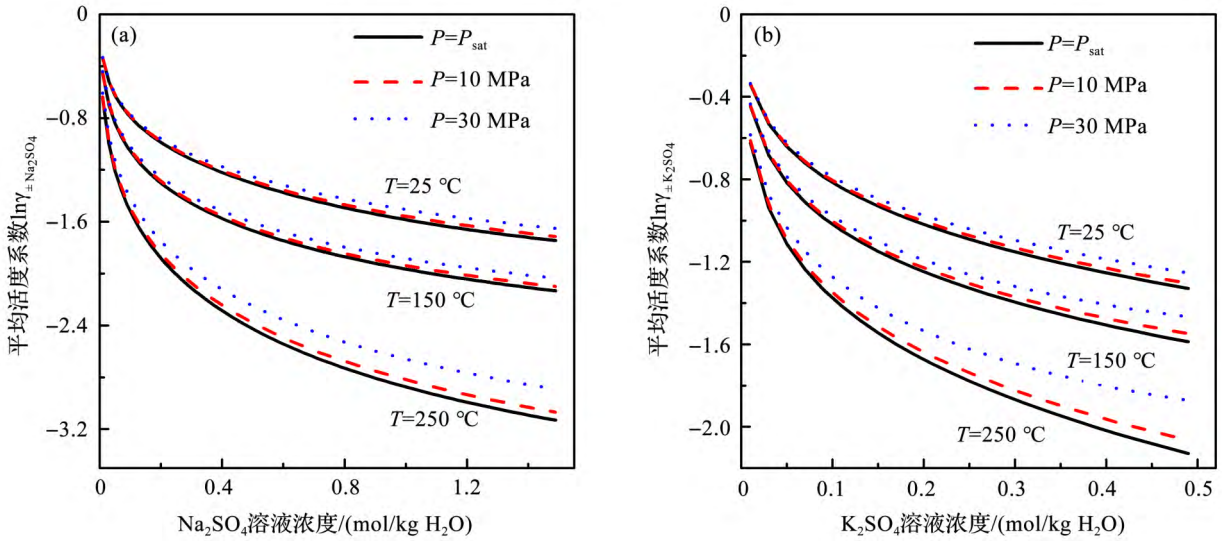

图 4　不同温度压力下模型计算的 Na_2SO_4（a）和 K_2SO_4（b）平均活度系数随浓度的变化

Fig. 4　The model calculated Na_2SO_4 (a) and K_2SO_4 (b) mean activity coefficient as a function of concentration at different temperature and pressure

获得了压力对 Na_2SO_4 和 K_2SO_4 的标准摩尔体积和活度系数的影响之后，依据公式（4）和公式（5）计算了水热体系中 Na_2SO_4 和 K_2SO_4 的溶度积和溶解度。从表 4 可以看出，模型计算的结果和实验测得的溶解度之间吻合较好。对于 Na_2SO_4 体系，Voisin 等[60]研究了压力为 25 MPa 时，水热体系中 Na_2SO_4 溶解度随温度的变化，并给出了计算 Na_2SO_4 溶解度的经验公式。从表 4 我们发现，本文模型计算的 Na_2SO_4 溶解度与 Voisin 等[60]经验公式计算的结果吻合较好。但是对于 K_2SO_4 体系，高压的实验数据基本都是在超临界条件以上，只能和饱和蒸汽压的实验室数据对比。

图 5 和图 6 分别表示水热体系模型计算的 Na_2SO_4 和 K_2SO_4 的溶度积的自然对数和溶解度。从图 5a 中可以看出，压力能够促进电解质溶解平衡常数的增加，在 150 ℃，压力为饱和蒸气压，10 MPa 和 30 MPa 时，Na_2SO_4 溶解平衡常数的自然对数分别为 −2.71，−2.65 和 −2.55；相同条件下 K_2SO_4 溶度积的自然对数分别为 −3.50，−3.45 和 −3.36（图 6a）。但是压力对电解质溶解度的影响，却恰好与之相反。从图 5b 中可以看出，随着压力的增大，电解质的溶解度却迅速降低。150 ℃时，随着压力的增加，Na_2SO_4 的溶解度从饱和蒸气压的 2.89 mol/kg 降低到 10 MPa 的 2.73 mol/kg，最后降低到 30 MPa 的 2.48 mol/kg。在相同温压条件下，K_2SO_4 的溶解度分别为 1.57，1.26 和 1.00 mol/kg。随着温度的升高，溶解度的减少量更大（图 6b）。这是因为压力对 Na_2SO_4 和 K_2SO_4 的溶度积和平均活度系数都有正向的促进作用，但是压力对 Na_2SO_4 和 K_2SO_4 平均活度系数的影响更明显，结果就导致了 Na_2SO_4 和 K_2SO_4 溶解度的降低。

表 4　模型计算的 Na_2SO_4 和 K_2SO_4 溶解度和实验结果的对比

Table 4　Comparison between model calculated Na_2SO_4 and K_2SO_4 with experimental data

	温度/℃	实验结果/（mol/kg）	模型计算/（mol/kg）	参考文献
Na_2SO_4 $P=P_{sat}$	60.0	3.15	3.34	[16,27]
	100.0	2.99	3.04	
	120.0	2.95	2.94	
	140.7	2.96	2.89	
	200.7	3.15	3.16	
K_2SO_4 $P=P_{sat}$	50.00	0.95	0.94	[15]
	80.00	1.23	1.20	
	100.0	1.40	1.33	
	150.0	1.69	1.57	
	190.0	1.97	1.71	
Na_2SO_4 P= 25 MPa	50.0	3.53	3.19	[60]
	100.0	2.34	2.74	
	150.0	2.33	2.53	
	180.0	2.39	2.48	
	200.0	2.41	2.46	
	220.0	2.37	2.40	

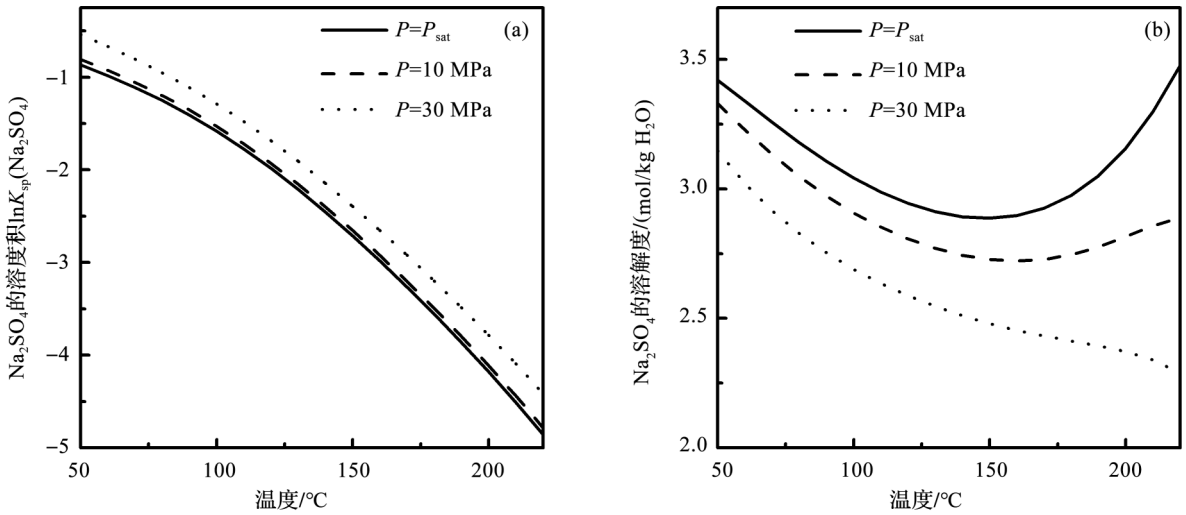

图5 Na_2SO_4溶解平衡常数的自然对数(a)和溶解度(b)随温度压力的变化

Fig.5 The natural logarithm of Na_2SO_4 solubility product (a) and solubility (b) at different temperature and pressure

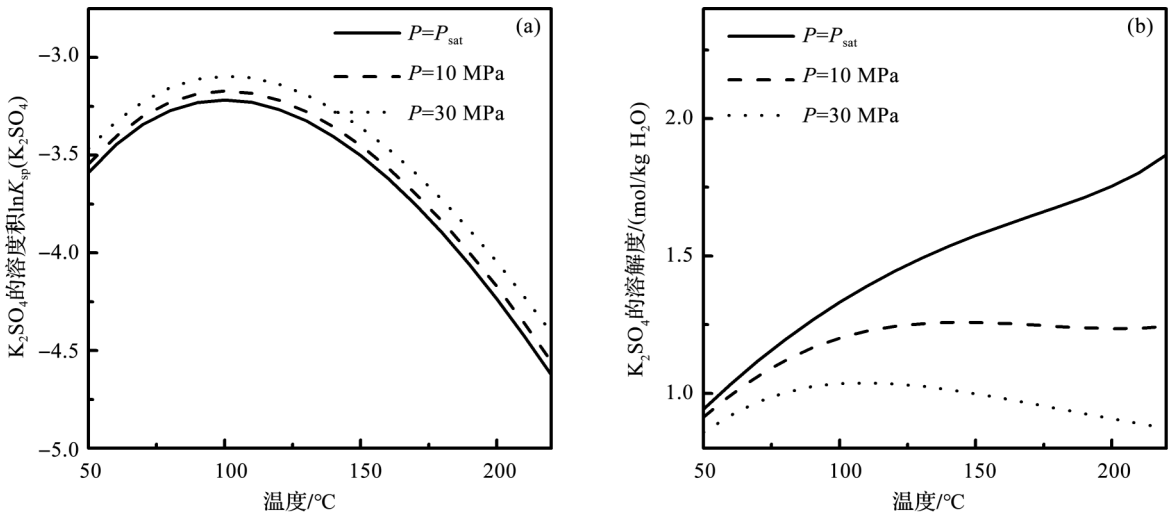

图6 K_2SO_4溶解平衡常数的自然对数(a)和溶解度(b)随温度压力的变化

Fig.6 The natural logarithm of K_2SO_4 solubility product (a) and solubility (b) at different temperature and pressure

4 结 论

本文使用Pitzer模型,利用水热体系中Na_2SO_4和K_2SO_4溶液的密度数据,使用非线性最小二乘法拟合,获得了Pitzer模型表示的Na_2SO_4和K_2SO_4的活度系数以及$Na_2SO_{4(aq)}$和$K_2SO_{4(aq)}$的标准偏摩尔体积随压力变化的模型参数,评价了压力对Na_2SO_4和K_2SO_4的溶度积和活度系数的影响,结果显示压力对Na_2SO_4和K_2SO_4的平均活度系数和溶度积都有正向的促进作用,但是压力对活度系数的影响更大。在此基础上构建了温度到250 ℃,压力到40 MPa的Na_2SO_4和K_2SO_4溶解度计算模型。模型计算的Na_2SO_4和K_2SO_4溶解度与已发表文献中的实验数据吻合较好。计算结果显示,Na_2SO_4和K_2SO_4的溶解度随压力的增大而降低,并且随着温度的升高降低的程度也变得更大。

参考文献(References):

[1] Xiao Rongge, Zhang Zongheng, Chen Huiquan, *et al*. Types of geological fluids and ore-forming fluid [J]. *Earth Science Frontiers*, 2001, 8(4): 245-251.[肖荣阁, 张宗恒, 陈卉泉, 等. 地质流体自然类型与成矿流体类型[J]. 地学前缘, 2001, 8(4): 245-251.]

[2] Xie Yuling, Tian Shihong, Hou Zengqian, *et al*. Discussion of migration and precipitation mechanics in Muluo REE deposit

Miannong country, west Sichuan Province: Evidence from fluid inclusion in bastnaeite [J]. *Acta Petrologica Sinica*, 2008, 24(3):555-561.[谢玉玲，田世洪，侯增谦，等. 四川冕宁木落稀土矿床稀土元素迁移与沉淀机制：来自稀土矿物中流体包裹体的证据[J]. 2008, 24(3):555-561.]

[3] Li Yongqiang. The Coexistence and Symbiosis Relation Research of Jinding Large-Scale Lead Zinc and the Sulfate Ore Deposit [D]. Xi'an: Changan University, 2006.[李永强. 兰坪金顶超大型铅锌矿床与硫酸盐矿床共存共生关系研究[D]. 西安：长安大学，2006.]

[4] Xu Jinhong, Zhang Zhengwei, Yang Xiaoyong, *et al*. The low-temperature mineralization of structurally-controlled fluids in Dahegou antimony ore deposit, Henan Province [J]. *Acta Geologica Sinica*, 2017, 91(12): 2 739-2 756.[徐进鸿，张正伟，杨晓勇，等. 河南省大河沟锑矿床构造—流体与低温成矿[J]. 地质学报，2017，91(12)：2 739-2 756.]

[5] Lu Huanzhang, Fan Hongrui, Ni Pei, *et al*. Fluind inclusion [M]. Beijing: Science Press, 2004.[卢焕章，范宏瑞，倪培，等. 流体包裹体[M]. 北京：科学出版社，2004.]

[6] Frezzotti M L, Tecce F, Casagli A. Raman spectroscopy for fluid inclusion analysis [J]. *Journal of Geochemical Exploration*, 2012, 112(1): 1-20.

[7] Li Xiaochun, Fan Hongrui, Hu Fangfang, *et al*. An analysis of the invidual fluid inclusion by LA-ICP-MS and its application to ore deposit [J]. *Mineral Deposit*, 2010, 29(6): 1 017-1 028.[李晓春，范宏瑞，胡芳芳，等. 单个流体包裹体LA-ICP-MS成分分析及在矿床学中的应用[J]. 矿床地质，2010，29(6)：1 017-1 028.]

[8] Sun He, Xiao Yilin. Fluid inclusion: Latest development, geological application and prospect [J]. *Advances in Earth Science*, 2009, 24(10): 1 105-1 121.[孙贺，肖益林. 流体包裹体研究：进展、地质应用及展望[J]. 地球科学进展，2009，24(10)：1 105-1 121.]

[9] Yao Ying, Sun Qiang. Raman quantitative measurements for carbon isotopic composition in CO_2-rich fluid inclusion: A preliminary study [J]. *Advances in Earth Science*, 2016, 31(10): 1 032-1 040.[药瑛，孙樯. 应用于流体包裹体CO_2碳同位素组成的拉曼光谱定量研究探讨[J]. 地球科学进展，2016，31(10)：1 032-1 040.]

[10] Wei Qing, Fan Hongrui, Lan Tingguang, *et al*. Genesis of Sizhuang gold deposit, Jiaodong peninsula: Evidences from fluid inclusion and quartz solubility modeling [J]. *Acta Petrologica Sinica*, 2015, 31(4): 1 049-1 062.[卫清，范宏瑞，蓝廷广，等. 胶东寺庄金矿床成因：流体包裹体与石英溶解度证据[J]. 岩石学报，2015，31(4)：1 049-1 062.]

[11] Chi Guoxiang, Lai Jianqing. Roles of fluid inclusion in study of mineral deposit [J]. *Mineral Deposit*, 2009, 28(6): 850-855.[池国祥，赖健清. 流体包裹体在矿床研究中的作用[J]. 矿床地质，2009，28(6)：850-855.]

[12] Xu Wengang, Fan Hongrui. Ore-forming fluids of the oxidized and reduced porphyry deposits [J]. *Earth Science Frontiers*, 2011, 18(5): 103-120.[徐文刚，范宏瑞. 氧化性和还原性斑岩型矿床流体成矿特征分析[J]. 地学前缘，2011，18(5)：103-120.]

[13] Xie Yuling, Hou Zengqian, Yin Shuping, *et al*. Continuous carbonatitic melt-fluid evolution of a REE mineralization system: Evidence from inclusions in the Maoniuping REE deposit, Western Sichuan, China [J]. *Ore Geology Reviews*, 2009, 36(1): 90-105.

[14] Linke W F. Solubilities of Inorganic and Metalorganic Compounds (4th ed) [M]. Washington: American Chemical Society, 1965.

[15] Eysseltová J, Bouaziz R. IUPAC-NIST solubility data series. 93. Potassium sulfate in water [J]. *Journal of Physical and Chemical Reference Data*, 2012, 41(1): 0131031. DOI: 10.1002/chin.201340220.

[16] Schroeder W C, Gabriel A, Partridge E P. Solubility equilibria of sodium sulfate at temperatures of 150 to 350 °C. I. Effect of sodium hydroxide and sodium chloride [J]. *Journal of the American Chemical Society*, 1935, 57(9): 1 539-1 546.

[17] Ding X, Zhang T, Zhang S, *et al*. Experimental determination and modelling of the solubilities of sodium sulfate and potassium sulfate in sub-and supercritical water [J]. *Fluid Phase Equilibria*, 2019, 483: 31-51.

[18] Dipippo M M, Sako K, Tester J W. Ternary phase equilibria for the sodium chloride-sodium sulfate-water system at 200 and 250 bar up to 400 °C [J]. *Fluid Phase Equilibria*, 1999, 157(2): 229-255.

[19] Leusbrock I, Metz S J, Rexwinkel G, *et al*. Quantitative approaches for the description of solubilities of inorganic compounds in near-critical and supercritical water [J]. *The Journal of Supercritical Fluids*, 2008, 47(2): 117-127.

[20] Mao S, Peng Q, Wang M, *et al*. The PVTx properties of aqueous electrolyte solutions containing Li^+, Na^+, K^+, Mg^{2+}, Ca^{2+}, Cl^- and SO_4^{2-} under conditions of CO_2 capture and sequestration [J]. *Applied Geochemistry*, 2017, 86: 105-120.

[21] Duan Zhenhao. State equation of geological fluid [J]. *Science in China*(*Series D*), 2010, 40(4): 393-413.[段振豪. 地质流体状态方程[J]. 中国科学：D辑，2010，40(4)：393-413.]

[22] Zhong R, Brugger J, Tomkins A G, *et al*. Fate of gold and base metals during metamorphic devolatilization of a pelite [J]. *Geochimica et Cosmochimica Acta*, 2015, 171: 338-352.

[23] Pan Aoran, Shan Huimei, Peng Sanxi, *et al*. Thermodynamic modeling of thioarsenic species distribution in high As groundwater in Hetao Plain [J]. *Advances in Earth Science*, 2018, 33(11): 1 169-1 180.[潘敖然，单慧媚，彭三曦，等. 基于热力学模拟河套平原高砷地下水中硫代砷形态分布特征[J]. 地球科学进展，2018，33(11)：1 169-1 180.]

[24] Hu Q C, Guo H R, Lu X B, *et al*. Determination of P-V-T-x properties of the CO_2-H_2O system up to 573.15 K and 120 MPa-experiments and model [J]. *Chemical Geology*, 2016, 424: 60-72.

[25] Mao S, Duan Z. The P, V, T, x properties of binary aqueous chloride solutions up to T = 573 K and 100 MPa [J]. *The Journal of Chemical Thermodynamics*, 2008, 40(7): 1 046-1 063.

[26] Greenberg J P, Møller N. The prediction of mineral solubilities in natural waters: A chemical equilibrium model for the Na-K-Ca-Cl-SO_4-H_2O system to high concentration from 0 to 250 °C [J]. *Geochimica et Cosmochimica Acta*, 1989, 53(10): 2 503-2 518.

[27] Pabalan R T, Pitzer K S. Thermodynamics of concentrated electrolyte mixtures and the prediction of mineral solubilities to high temperatures for mixtures in the system Na-K-Mg-Cl-SO_4-OH-H_2O [J]. *Geochimica et Cosmochimica Acta*, 1987, 51

(9): 2 429-2 443.

[28] Pitzer K S. Thermodynamics of electrolytes. I. Theoretical basis and general equations [J]. *The Journal of Physical Chemistry*, 1973, 77(2): 268-277.

[29] Wang L, Zhang W, Yang B, *et al*. Solubility measurements in Na-F-CO_3-HCO_3-H_2O system at (308.15 and 323.15) K and development of a Pitzer-based equilibrium model for the Na-F-Cl-SO_4-CO_3-HCO_3-H_2O system[J]. *The Journal of Chemical Thermodynamics*, 2019, 131: 88-96.

[30] Parkhurst D L, Appelo C A J. Description of Input and Examples for PHREEQC Version 3: A Computer Program for Speciation, Batch-Reaction, One-Dimensional Transport, and Inverse Geochemical Calculations [R]. U.S. Geological Survey, 2013.

[31] Kulik D A, Wagner T, Dmytrieva S V, *et al*. GEM-Selektor geochemical modeling package: Revised algorithm and GEMS3K numerical kernel for coupled simulation codes [J]. *Computational Geosciences*, 2013, 17(1): 1-24.

[32] Dai Z, Kan A, Zhang F, *et al*. A thermodynamic model for the solubility prediction of barite, calcite, gypsum, and anhydrite, and the association constant sstimation of $CaSO_4^{(0)}$ ion pair up to 250 °C and 22000 psi [J]. *Journal of Chemical and Engineering Data*, 2015, 60(3): 766-774.

[33] Shi W, Kan A, Fan C, *et al*. Solubility of barite up to 250 °C and 1500 bar in up to 6 m NaCl solution [J]. *Industrial and Engineering Chemistry Research*, 2012, 51(7): 3 119-3 128.

[34] Dai Z, Kan A, Shi W, *et al*. Calcite and barite solubility measurements in mixed electrolyte solutions and development of a comprehensive model for water-mineral-gas equilibrium of the Na-K-Mg-Ca-Ba-Sr-Cl-SO_4-CO_3-HCO_3-$CO_{2(aq)}$-H_2O System up to 250 °C and 1500 bar [J]. *Industrial and Engineering Chemistry Research*, 2017, 56 (23): 6 548-6 561.

[35] Millero F J. The effect of pressure on the solubility of minerals in water and seawater [J]. *Geochimica et Cosmochimica Acta*, 1982, 46(1): 11-22.

[36] Appelo C A J, Parkhurst D L, Post V E A. Equations for calculating hydrogeochemical reactions of minerals and gases such as CO_2 at high pressures and temperatures [J]. *Geochimica et Cosmochimica Acta*, 2014, 125: 49-67.

[37] Monnin C. A thermodynamic model for the solubility of barite and celestite in electrolyte solutions and seawater to 200 °C and to 1 kbar [J]. *Chemical Geology*, 1999, 153(1/4): 187-209.

[38] Robie R A, Hemmingway B, Fisher J R. Thermodynamic Properties of Minerals and Related Substances at 298.15 K and 1 bar (10^5 pascals) Pressure and at Higher Temperature [R]. Denver, CO: U.S. Geological Survey, 1978.

[39] Rogers P S Z, Pitzer K S. Volumetric properties of aqueous sodium vhloride solutions [J]. *Journal of Physical and Chemical Reference Data*, 1982, 11(1): 15-81.

[40] Pitzer K S, Peiper J C, Busey R H. Thermodynamic properties of aqueous sodium chloride solutions [J]. *Journal of Physical and Chemical Reference Data*, 1984, 13(1): 1-102.

[41] Königsberger E, Eriksson G, May P M, *et al*. Comprehensive model of synthetic Bayer liquors. Part 1. Overview [J]. *Industrial and Engineering Chemistry Research*, 2005, 44(15): 5 805-5 814.

[42] Wagner W, Kruse A, Kurtzschmar H J. Properties of Water and steam: The Industrial Standard IAPWS-IF97 for the Thermodynamic Properties and Supplementary Equations for Other Properties: Tables Based on These Equations [M]. Berlin: Springer-Verlag Berlin, 1998.

[43] Pabalan R T, Pitzer K S. Thermodynamics of $NaOH_{(aq)}$ in hydrothermal solutions [J]. *Geochimica et Cosmochimica Acta*, 1987, 51(4): 829-837.

[44] Bradley D J, Pitzer K S. Thermodynamics of electrolytes. 12. Dielectric properties of water and Debye-Hückel parameters to 350 °C and 1 kbar [J]. *Journal of Physical Chemistry*, 1979, 83(12): 1 599-1 603.

[45] Archer D G. Thermodynamic properties of the KCl+H_2O system [J]. *Journal of Physical and Chemical Reference Data*, 1999, 28(1): 1-17.

[46] Rowland D, May P M. A Pitzer-based characterization of aqueous magnesium chloride, calcium chloride and potassium iodide solution densities to high temperature and pressure [J]. *Fluid Phase Equilibria*, 2013, 338: 54-62.

[47] Møller N. The prediction of mineral solubilities in natural waters: A chemical equilibrium model for the Na-Ca-Cl-SO_4-H_2O system, to high temperature and concentration [J]. *Geochimica et Cosmochimica Acta*, 1988, 52(4): 821-837.

[48] Obšil M, Majer V, Hefter G T, *et al*. Densities and apparent molar volumes of $Na_2SO_{4(aq)}$ and $K_2SO_{4(aq)}$ at temperatures from 298 K to 573 K and at pressures up to 30 MPa [J]. *Journal of Chemical and Engineering Data*, 1997, 42(1): 137-142.

[49] Al Ghafri S Z, Maitland G C, Trusler J P M. Densities of $SrCl_{2(aq)}$, $Na_2SO_{4(aq)}$, $NaHCO_{3(aq)}$, and two synthetic reservoir brines at temperatures between (298 and 473) K, pressures up to 68.5 MPa, and molalities up to 3 mol·kg^{-1} [J]. *Journal of Chemical and Engineering Data*, 2013, 58(2): 402-412.

[50] Apelblat A, Manzurola E, Orekhova Z. Thermodynamic properties of aqueous electrolyte solutions. volumetric and compressibility studies in 0.1 mol·kg^{-1}, 0.5 mol·kg^{-1}, and 1.0 mol·kg^{-1} sodium carbonate and sodium sulfate solutions at temperatures from 278.15 K to 323.15 K [J]. *Journal of Chemical and Engineering Data*, 2009, 54(9): 2 550-2 561.

[51] Saluja P P S, Pitzer K S, Phutela R C. High-temperature thermodynamic properties of several 1:1 electrolytes [J]. *Canadian Journal of Chemistry*, 1986, 64(7): 1 328-1 335.

[52] Chen C T, Emmet R T, Millero F J. The apparent molal volumes of aqueous solutions of sodium chloride, potassium chloride, magnesium chloride, sodium sulfate, and magnesium sulfate from 0 to 1000 bars at 0, 25, and 50 °C [J]. *Journal of Chemical and Engineering Data*, 1977, 22(2): 201-207.

[53] Ellis A J. Partial molal volumes in high-temperature water. Part III. halide and oxyanion salts [J]. *Journal of the Chemical Society A: Inorganic, Physical, Theoretical*, 1968. DOI: 10.1039/j19680001138.

[54] Saluja P P S, Lemire R J, Leblanc J C. High-temperature thermodynamics of aqueous alkali-metal salts [J]. *The Journal of Chemical Thermodynamics*, 1992, 24(2): 181-203.

[55] Zezin D, Driesner T, Sanchez-Valle C. Volumetric properties of Na_2SO_4-H_2O and Na_2SO_4-NaCl-H_2O solutions to 523.15 K, 70 MPa [J]. *Journal of Chemical and Engineering Data*, 2015, 60(4): 1 181-1 192.

[56] Azizov N D, Akhundov T S. The bulk properties of the Na_2SO_4-

H_2O system in a wide range of the parameters of state [J]. *High Temperature*, 2000, 38(2): 203-209.

[57] Laliberté M. A model for calculating the heat capacity of aqueous solutions, with updated density and viscosity Data [J]. *Journal of Chemical and Engineering Data*, 2009, 54(6): 1 725-1 760.

[58] Azizov N D. The density and partial properties of K_2SO_4-H_2O solutions from room temperature to 573 K [J]. *Zhurnal Neorganicheskoi Khimii*, 1998, 43(2): 323-327.

[59] Pearce J N, Eckstrom H C. Vapor pressures and partial molal volumes of aqueous solutions of the alkali sulfates at 25° [J]. *Journal of the American Chemical Society*, 1937, 59(12): 2 689-2 691.

[60] Voisin T, Erriguible A, Philippot G, *et al*. Investigation of the precipitation of Na_2SO_4 in supercritical water [J]. *Chemical Engineering Science*, 2017, 174: 268-276.

Thermodynamic Calculation of Solubility of Na_2SO_4/K_2SO_4 in Hydrothermal Fluids*

Zhang Wei[1,2], Zhou Li[2*], Tang Hongfeng[2], Li Heping[2], Wang Li[2,3]

(1.*Research Center of Karst Ecological Civilization*, *Guizhou Normal University*, *Guiyang* 550025, *China*; 2.*Key Laboratory of High-Temperature and High-Pressure Study of the Earth's Interior*, *Institute of Geochemistry*, *Chinese Academy of Sciences*, *Guiyang* 550002, *China*; 3.*University of Chinese Academy of Sciences*, *Beijing* 100039, *China*)

Abstract: Sulfate fluids are common fluids in nature, and their salinity studies can provide important information for the evolution of ore-forming fluids, migration and enrichment of ore-forming elements, and the classification of deposit types. Considerable research has been carried out to investigate the solubility of Na_2SO_4 and K_2SO_4 in hydrothermal fluids, however most of the literature reported experimental data were under saturated vapor pressure or the water supercritical region. A few data have been reported for the low temperature hydrothermal mineralization region. Thermodynamic model is a useful method to study the properties of hydrothermal geofluids, especially for mineral solubility. Pitzer interaction model is one of the most widely used model to calculate the thermodynamic properties of hydrothermal fluids, but few work have ever been carried out to calculate the solubility of sulfate at high temperature and pressure. With Pitzer specific interaction model, using the literature reported density data of Na_2SO_4 and K_2SO_4 solutions at high temperature and pressure, the pressure effect on Pitzer activity coefficient of sulfate and the standard partial molar volume change during sulfate dissolution process were evaluated and related parameters were obtained. The standard partial molar volumes of Na_2SO_4 and K_2SO_4 calculated with these parameters agreed well with those reported in the literature. Combined with the relevant parameters in the literature under saturated vapor pressure, a thermodynamic model for Na_2SO_4 and K_2SO_4 solubility calculation with temperature up to 250 ℃ and pressure up to 40 MPa was developed. The model gave very good agreement with the experimental solubility data. With this model, Na_2SO_4 and K_2SO_4 solubility was calculated at high temperature and pressure. The calculation results showed that pressure had a positive effect on both the average activity coefficient and solubility product of Na_2SO_4 and K_2SO_4, but the solubility of Na_2SO_4 and K_2SO_4 decreased with pressure due to the larger change of the average activity coefficient with pressure. And as the temperature increased, the degree of such reduction became larger. The results herein can provide instructions for the compositional analysis of sulfate fluid inclusions.

Key words: Sulfate fluids inclusion; Solubility; Thermodynamic model; Pitzer model.

* **Foundation item:** Project supported by the National Natural Science Foundation of China "Experimental study of the behavior of monazite and xenotime in hydrothermal fluids: Constraints on the usefulness of U-Th-Pb age and the mineralization of REE" (No. 41773058); The Joint Foundation of Guizhou Science and Technology Department and Guizhou Normal University "Study on sustainable utilization of geothermal resources in Shiqian County" (No. QIANKEHE LH [2017] 7339).

First author: Zhang Wei(1988-), male, Wuhan City, Hubei Province, Lecturer. Research areas include experimental and computational geochemistry on water-rock reactions. **E-mail**:zhangwei@gznu.edu.cn

* **Corresponding author:** Zhou Li (1980-), male, Qianjiang City, Hubei Province, Associate professor. Research areas include experimental geochemistry at high-temperature and high pressure. **E-mail**:zhouli@vip.gyig.ac.cn